Third Order LPF Type Compensator for Flexible Rotor Suspension

O. MATSUSHITA, N. TAKAHASHI AND M. TAKAGI

ABSTRACT

The tuning job of the compensator for levitating flexible rotors supported by active magnetic bearings (AMB) concerns providing good damping effect to the critical speed modes while avoiding the spillover problem on the instability of higher bending modes. In this paper, an idea for design of the control law of the compensator based on utilizing a third order low pass filter (LPF) is proposed to essential enable elimination of the spillover instability. According to the proposed design method, good damping effects for the critical speeds are obtained by the usual phase lead/lag function. Stabilization for all of higher bending modes is completed by the additional function of the 3rd order LPF due to its phase lag approaching about -270 degree in the high frequency domain. This idea is made clear by experiments and simulations.

INTRODUCTION

To design control network driving active magnetic bearings (AMB) for flexible rotor levitation, it is important to consider rigid mode levitation, controllability of flexible modes at critical speeds and stability margin for high frequency bending modes. For instance, a design of super critical compressors supported by AMBs illustrates this point. In the first design phase, rigid mode levitation performance is determined. Next, well damping ratio of the first bending mode necessary to pass the critical speed is determined according to Q-value criteria. Finally, the PID controller transfer function is tuned so as to satisfy these two requirements and so as to avoid higher frequency instability beyond 2nd bending modes. It is called a spillover problem.

Usually, the PID control law with optional notch filters and/or low pass filters is used for tuning. Otherwise, the increase of the internal damping of the rotor is improved. However, this design method based upon the phase lead/lag function is not free from the spillover problem. However, the presented method can provide a highly robust control system for the higher modes and satisfactory performance for the controlled modes. It is possible to skillfully combine the commonly used phase lead/lag function with the 3rd order LPF. How to design the 3rd order LPF is a main point of this paper.

The phase lead/lag function can possibly provide enough damping performance to the rigid and first bending modes. It can be done by placing these critical speeds in the phase lead domain.

Osami Matsushita and Naohiko Takahashi : Tsuchiura Works, Hitachi, Ltd.,
603 Kandatsu-machi Tsuchiura-shi Ibaraki JAPAN 300
Michiyuki Takagi : Mechanical Engineering Research Laboratory, Hitachi, Ltd., ibid.

The proposed design method features the addition of the 2nd order LPF within this 3rd order LPF. The center frequency of the 2nd order LPF coincides with the eigen frequency of the rotor restricted by pin-pin boundary at AMB portions. This eigen frequency is equal to the anti-resonance frequency located between the 1st and 2nd bending modes. Since the total function of the control function becomes a 3rd order LPF, the phase lag forwards to -270 degrees, i.e., 90 degree phase lead, in the high frequency domain. Therefore, all the higher natural frequencies beyond the 2nd bending mode are essentially stable, i.e., completely free from the spillover problem.

This idea is theoretically explained for a rotor system with one AMB support. The effectiveness of this design method is proven by numerical simulations and experimental results. The rotation test is done with a low enough Q-value to pass the rigid and first bending critical speed without the high frequency instability. The generalization of this design concept is finally proposed for the rotor borne by two AMBs.

A FLEXIBLE ROTOR WITH ONE ACTIVE MAGNETIC BEARING

A flexible rotor shown in Fig.1 is selected for explaining the fundamental idea of the design method of AMB compensator. The rotor is supported by a ball bearing at the right end and by an AMB at the other. The ball bearing placed here is represented by the pin boundary condition to explain the idea clearly. The problem then focuses on to how to design the compensator deriving the AMB at the left side.

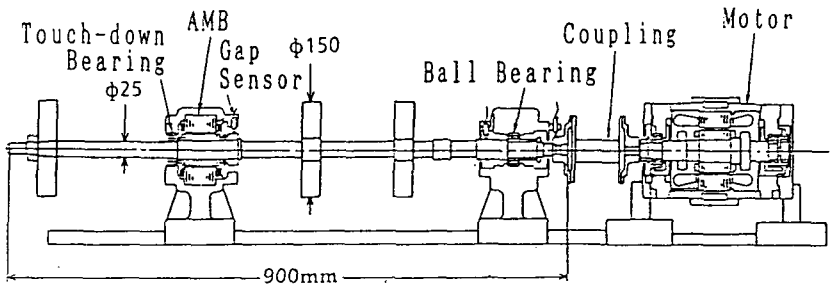

Fig.1 Experimental Test Rig

A gap sensor placed at the left side detects the rotor radial displacement which feeds its signal to the controller. The signal from the controller derives the magnetic bearing force through the power amplifier having a transfer function of unity. The rotor is connected to a motor with a flexible coupling. The flexible coupling is flexible enough to satisfy the free boundary condition at the right end of the rotor as shown Fig.2(a). Gyroscopic effects are neglected here.

The displacement vector is noted by $X=[X_1^t, X_2]$: X_2 for the rotor displacement at the AMB portion and X_1 for the displacements of all portions of the rotor except the AMB portion. The former is called the boundary displacement and the latter called the inner displacement vector. In the AMB servo-control system, the boundary displacement X_2 is measured and the AMB force U acts upon the rotor according to a control law. Then, the equation of motion of the rotor-bearing system can be written in matrix form as follows:

$$\begin{bmatrix} M_1 & \\ & M_2 \end{bmatrix} \begin{bmatrix} \ddot{X}_1 \\ \ddot{x}_2 \end{bmatrix} + \begin{bmatrix} K_{11} & K_{12} \\ K_{12}^t & K_{22} \end{bmatrix} \begin{bmatrix} X_1 \\ x_2 \end{bmatrix} = \begin{bmatrix} 0 \\ 1 \end{bmatrix} u \qquad (1)$$

where M_i and K_{ij} (i,j=1,2) indicate mass and stiffness matrices of the rotor system, respectively, noted by 1 for the inner portion and by 2 for the boundary AMB portion.

Any damping factors, e.g., shaft material damping, mechanical dampers, are neglected. In the authors' opinion, the consideration of such system damping factors, in addition, will potentially destroy the realization of practical robust control. Rotordynamics designers want to consider the compensator design for the AMB similarly the design for oil-film bearings, i.e., neglecting any system damping.

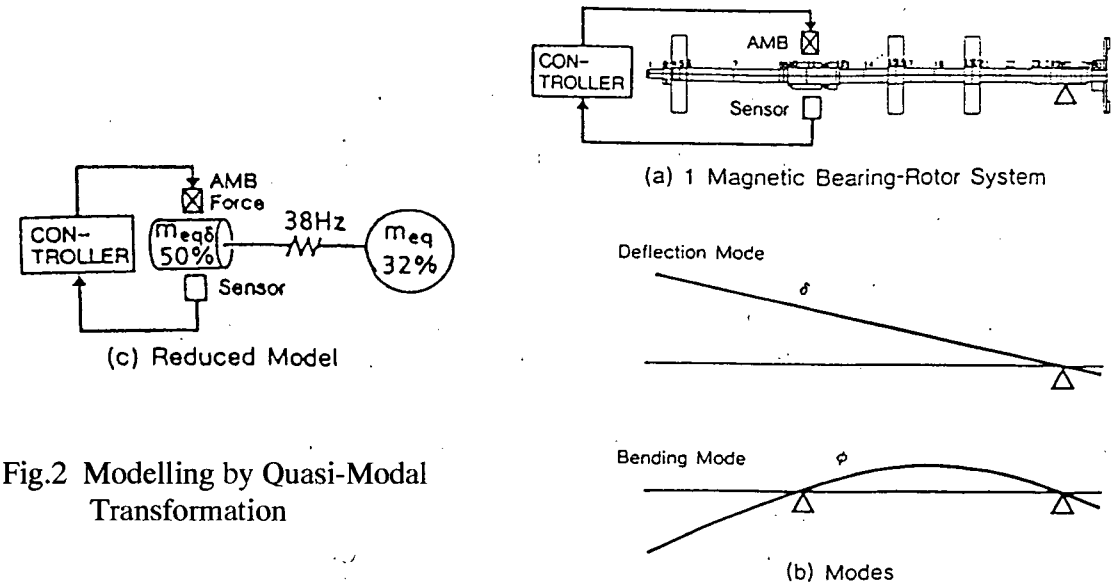

Fig.2 Modelling by Quasi-Modal Transformation

SYSTEM MODELLING

The equation of motion (1) of the rotor is formulated in FEM matrix forms on meshing by the shaft beam element. The quasi-modal system reduction in a category of the modal synthesis is applied to the original system. The quasi-modal transformation modes are determined by two kinds of modes as shown in Fig.2(b):

(1) Pure bending mode ϕ obtained by eigen mode of the rotor if the pin condition is imposed at the AMB portion.

(2) Rigid mode δ obtained by deflection mode if the rotor is lifted to give the unit displacement at the AMB portion.

The quasi-modal transformation is defined by the following equation

$$X=\begin{bmatrix} X_1 \\ x_2 \end{bmatrix}=\begin{bmatrix} \phi & \delta \\ 0 & 1 \end{bmatrix}\begin{bmatrix} s \\ x_2 \end{bmatrix} \tag{2}$$

where the variable s is a weighting value indicating the magnitude of the pure bending mode obtained in the rotor bending critical speed mode.

From the result of the transformation, the following equation of motion of the reduced model having 2 degrees of freedom is completed: [2,4]

$$\begin{bmatrix} m^* & m_c \\ m_c & m_\delta \end{bmatrix}\begin{bmatrix} \ddot{s} \\ \ddot{x}_2 \end{bmatrix}+\begin{bmatrix} k^* & \\ & 0 \end{bmatrix}\begin{bmatrix} s \\ x_2 \end{bmatrix}=\begin{bmatrix} 0 \\ 1 \end{bmatrix}u, \tag{3}$$

where $m^*=\phi^t M_1 \phi$, $m_c=\phi^t M_1 \delta$, $m_\delta=M_2+\delta^t M_1 \delta$, $k^*=m^* \omega_P^2$ and

ω_p = the natural frequency of the pure bending mode under the pin bounadry condition at the AMB portion.

This equation of motion having the mass interaction between the pure bending mode and the rigid mode is equivalently converted to the spring interaction. This conversion is possible to provide the reduced vibrating model visually composing the mass-spring connection, if a new absolute displacement z* is introduced as $s = a(x_1^* - x_2)$:

$$a = m_c / m^* = \phi^t M_1 \delta / \phi^t M_1 \phi \tag{4}$$

$$\begin{bmatrix} m_{eq} & \\ & m_{eq\delta} \end{bmatrix} \begin{bmatrix} \ddot{x}^* \\ \ddot{x}_2 \end{bmatrix} + \begin{bmatrix} k_{eq} & -k_{eq} \\ \text{sym.} & k_{eq} \end{bmatrix} \begin{bmatrix} x^* \\ x_2 \end{bmatrix} = \begin{bmatrix} 0 \\ 1 \end{bmatrix} u, \tag{5}$$

where $m_{eq}=a^2 m^*$, $m_{eq\delta}=m_\delta - m_{eq}$, $k_{eq}=m_{eq}\omega_p^2$ and $a=m_c/m^*=\phi^t M_1 \delta / \phi^t M_1 \phi$

The obtained model is illustrated in Fig.2(c). The masses of meq and meqδ indicate the equivalent masses of the rigid mode and the pure bending mode, respectively.

CONVENTIONAL DESIGN CONCEPT FOR COMPENSATOR [1,3]

The negative spring effect exhibited by the AMB is neglected. It can be easily compensated by certain gain of the proportional action. The equation of motion (5) of the model is rewritten by the state equation form as follows:

$$\begin{aligned} \dot{X} &= AX + bu \\ y &= cX \end{aligned} \tag{6}$$

where

$$X = \begin{bmatrix} x_2 \\ x^* \\ \dot{x}_2 \\ \dot{x}^* \end{bmatrix}, \quad A = \begin{bmatrix} 0 & 0 & 1 & 0 \\ 0 & 0 & 0 & 1 \\ -k_{eq}/m_{eq\delta} & k_{eq}/m_{eq\delta} & 0 & 0 \\ k_{eq}/m_{eq} & -k_{eq}/m_{eq} & 0 & 0 \end{bmatrix},$$

$$b = \begin{bmatrix} 0 \\ 0 \\ 1/m_{eq\delta} \\ 0 \end{bmatrix} \quad \text{and}$$

$$c = [\,1 \;\; 0 \;\; 0 \;\; 0\,]$$

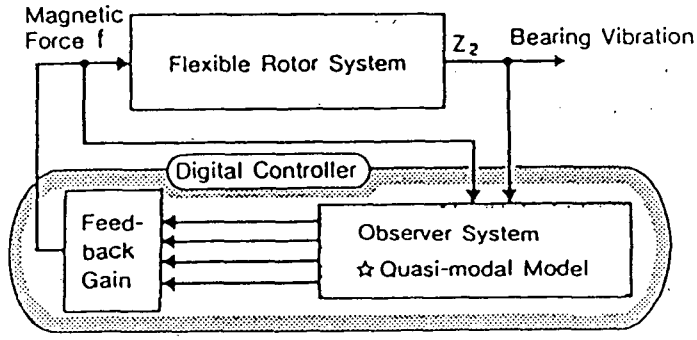

Fig. 3 Conventional Control Layout

The controller design based upon the modern control theory combining the full order observer and the optimum feedback gain due to LQR is applied to the model in the manner as shown in Fig.3. One example of the transfer function of the compensator itself is obtained as shown in Fig.4. The overall configuration of the transfer function is fundamentally similar to PID action, but down slope gain of 1st order LPF at the high frequency domain. Therefore, damping ratio of the rigid and first bending mode of the global system can be well provided. However, higher bending modes than the 2nd will be easily unstable due to the phase lag at this high frequency domain.

In fact, the phase curve on the Bode diagram changes from the phase lead region to the phase lag region beyond the peak portion of the gain curve. This phase lag forwarding to -90 degrees provides a negative damping effect for high frequency eigen modes of the global system. This is the reason why the spillover instability is induced.

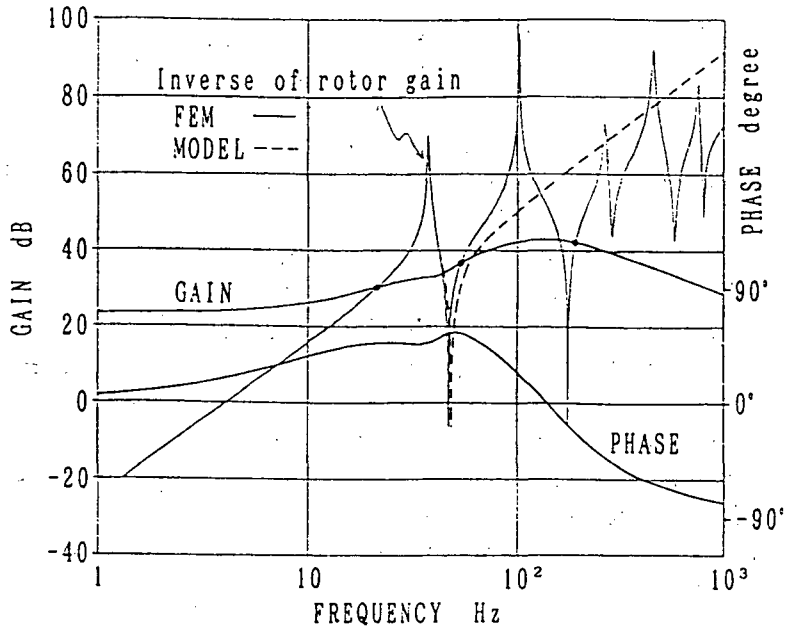

Fig.4 Controller Transfer Function (Conventional Design)

PROPOSED DESIGN CONCEPT FOR COMPENSATOR

The idea of the new design comes from the fact that if this phase lag forwards to -270 degrees instead of -90 degrees, the compensator can provide the positive damping to the system even in the high frequency domain. This idea can be realized by replacing the behavior of the 1st order LPF of the conventional compensator by one of the 3rd order LPF. In other words, it is easily completed by the cascade combination of the present type plus a 2nd order LPF as shown in Fig.5.

The type of the 2nd order LPF that must be added is now discussed. It is recommended that the center frequency of the 2nd order LPF is tuned with the anti-resonance frequency, i.e., the eigen frequency of the pure bending mode. This is because the rotor does not react to the resonance of the 2nd order LPF in the control network.

If the LQR method stated in APPENDIX is applied to a control objector, composing the rotor and this 2nd order LPF, this required compensator is automatically designed. One of the transfer functions of the proposed compensator is shown in Fig.6 including the 2nd order LPF. The dotted curve indicates the inverse function of rotor response against force input, called the rotor gain. The peak of the dotted curve indicates

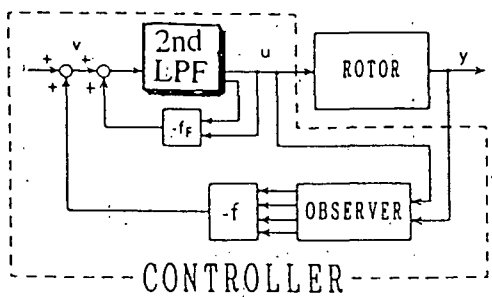

Fig.5 Control Layout (Proposed Design)

the anti-resonance frequency.

In this figure, the phase lead covers the natural frequency of the rigid and first bending modes to provide the well damping effects at the critical speeds. The phase lag starts beyond 80 Hz, but it quickly passes -180 degree before the 2nd bending mode and it finally moves forward to -270 degree. Therefore, positive damping is provided to all bending modes of the global system beyond the 2nd mode, ensuring stability. As obviously shown in this phase curve, all of the higher frequency modes are definitely stable. There is no spillover problem. This controller will be robust.

The result of the eigenvalue of the global system is shown in Tab.1. Clearly all modes are completely stabilized even with no material damping.

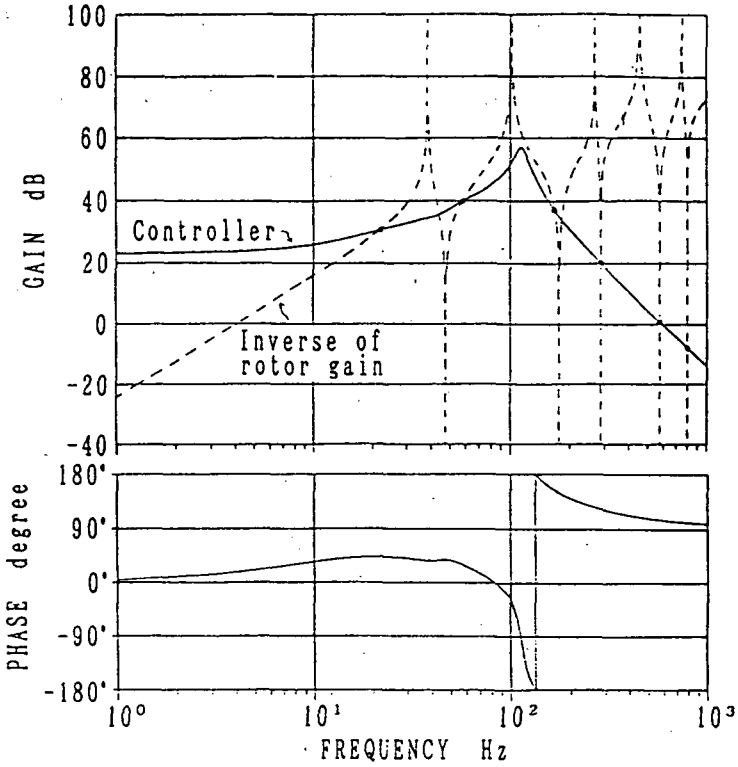

Fig.6 Controller Transfer Function(Proposed Design)

Table 1 Eigen values of the flexible rotor

Mode	Orpm eigen value (ζ %, Hz)	
	Open loop	Closed loop
Rigid mode	0, 0	61.65038, 20
1st bending mode	0, 47	16.24556, 48
2nd bending mode	0, 175	2.82522, 169
3rd bending mode	0, 285	0.05888, 285
4th bending mode	0, 374	0.00009, 374

EXPERIMENTAL RESULTS

A control law is made by digital means with the following specifications:

- Bilinear s-z transformation used for digitalization,
- 8 KHz for sampling frequency and
- DSP board (type ADSP320 made by Chubu Denki)

In the experiment, the integral action is added for statically levitating the rotor. A proportional action is also included in addition, for cancelling the negative spring effect in the AMB.

For experimentally checking the stability of the developed control law of the 3rd order LPF, it is compared with the commonly used PID control law as shown in Fig.7. In the case of the PID control, depending on the increase of the feedback loop gain, the instability of the 5th bending mode appears when the natural frequency of the rigid mode reaches 13 Hz. However, in the case of the 3rd LPF control, even if the rigid mode natural frequency is increased to 24 Hz, the bending mode instability does not appear. This proposed controller is thus very robust.

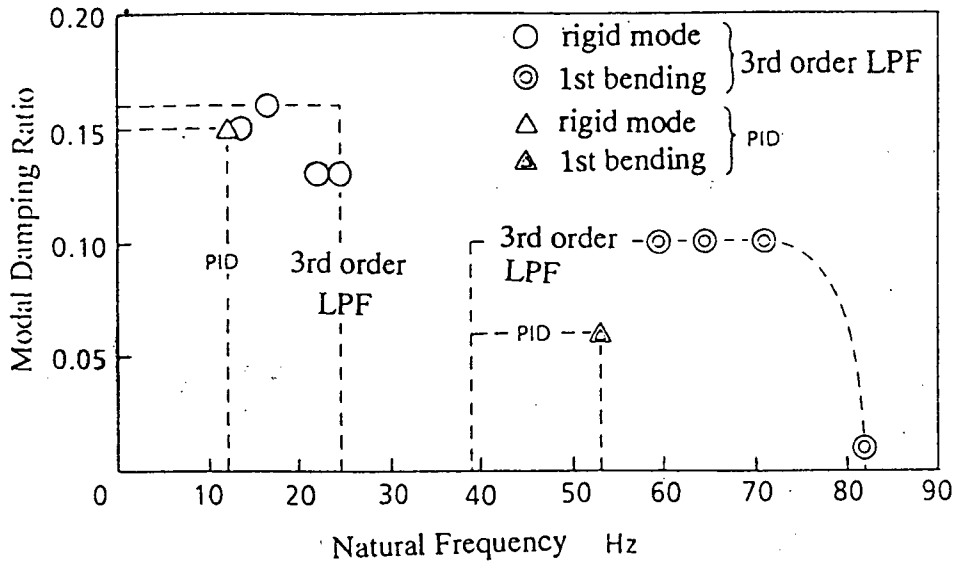

Fig.7 Comparison of Improvement of System Damping by Tuning

As shown in Fig.8, the vibration response curves are measured. Compared with the PID, enough damping effect is provided by the proposed controller for the rigid and first bending modes at the critical speeds. Small peak amplitudes are obtained compared with the conventional type.

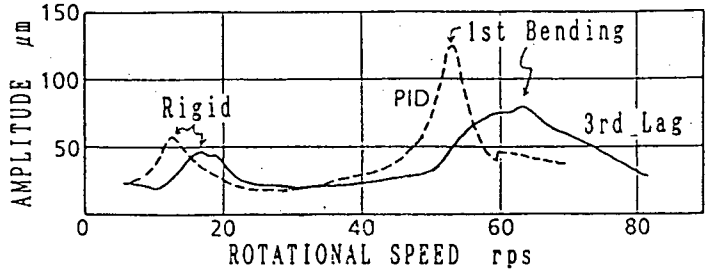

Fig.8 Vibration Response Curves

As suggested in Fig.9, test data prove the design concept is as follows:

- 1st eigen mode (rigid mode) and 2nd eigen mode (1st bending mode) can take enough damping ratio to pass the critical speeds owing to the phase lead. Consequently small Q-value design is completed.
- The higher eigen modes than the 3rd (2nd bending mode) are stabilized due to the phase lag of about -270 degrees. The spillover problem completely disappears for any higher frequency mode.
- The center frequency of the additional 2nd order LPF must be set with the anti-resonance frequency located between the 2nd and 3rd eigen modes (1 and 2nd bending modes). Even if the Q-value of the 2nd order LPF is high, the rotor does not react to such sensitivity as high as in the compensator network.

GENERALIZATION OF PROPOSED DESIGN CONCEPT

The rotor borne by two AMBs at the left and right sides is quite common. The concept of the compensator design developed for one AMB type can be enhanced to two AMB types. The natural frequency map is shown in Fig.10. On the left side of the map the natural frequency of the rotor subjected to free-free boundary condition is plotted. On the right side the natural frequency is that of the pin-pin boundary condition. The right side frequencies indicate anti-resonance frequencies.

For the type of two AMB there are two types of controller layouts: centralized and

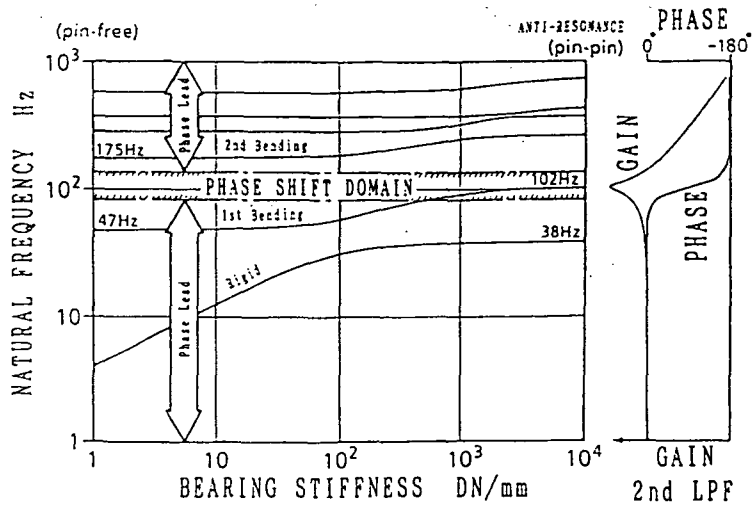

Fig.9 Natural Frequency Map (One AMB)

decentralized. The centralized layout employing the translation and tilting mode controls are suitable for the control law of the 3rd order LPF. The separation into both the modes and two independent compensators are prepared as shown in Fig.11.

According to this separation, two types of the compensator are independently designed, based on the design concept developed for the one AMB control :

- type 1 : translation mode compensator to control mainly the parallel rigid mode and the 1st bending mode of the rotor.
- type 2 : tilting mode compensator to control mainly the conical rigid mode and the 2nd bending mode of the rotor.

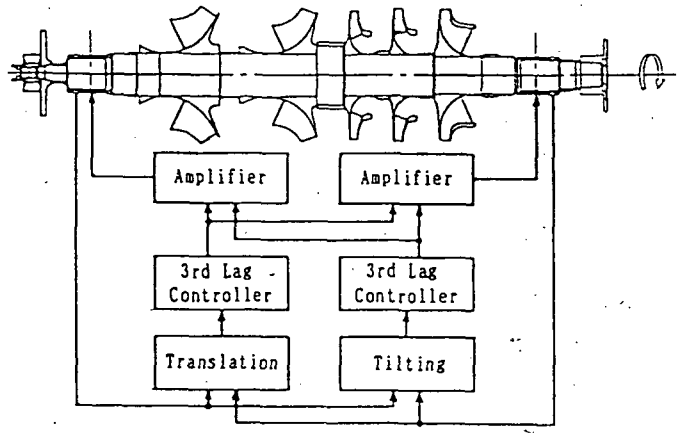

Fig.11 Centralized Controller Layout

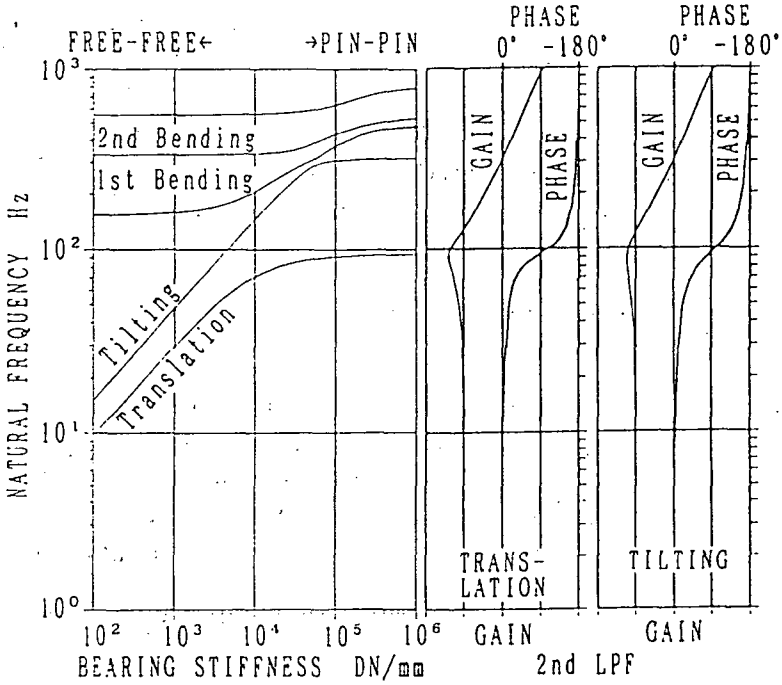

Fig.10 Natural Frequency Map (Two AMBs).

The obtained transfer functions of each compensator are shown in Fig.12 and 13. The center frequency of the 2nd order LPF coincides with the 1st anti-resonance frequency of the rotor under the pin-pin boundary condition, as shown in the natural frequency map of Fig.10.

The stability analysis of the global system is shown in Table 2. All of the bending modes are stabilized without spillover problems, even if no material damping. Clearly the completed regulators are very robust.

Table 2 Eigen values of the rotor (2 AMBs)

Mode	0rpm eigen value (ζ %, Hz)	
	Open loop	Closed loop
Translation mode	0, 0	26.66492, 29
Tilting mode	0, 0	18.48787, 31
1st bending mode	0, 154	2.93966, 152
2nd bending mode	0, 331	0.00290, 331
3rd bending mode	0, 555	0.00091, 555
4th bending mode	0, 786	0.00023, 786

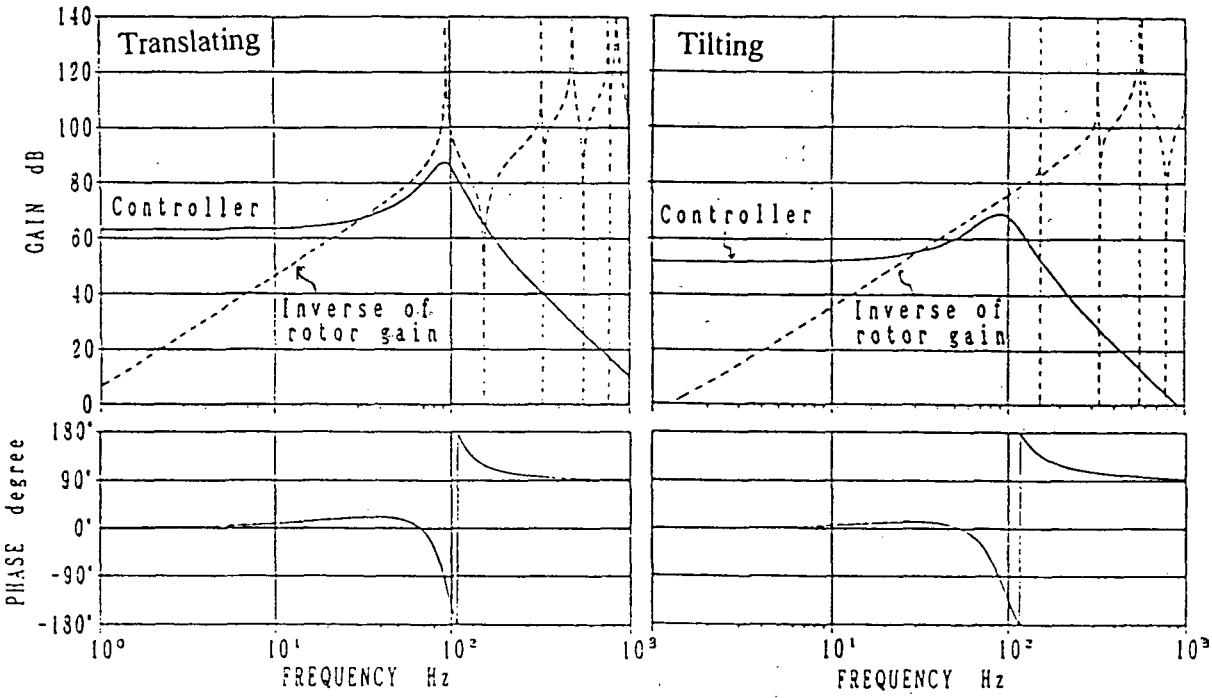

Fig.12 Transfer Function for Translating Mode Controller

Fig.13 Transfer Function for Tilting Mode Controller

CONCLUSION

A design concept for AMB control based on a 3rd order LPF is presented. It is a key point that the center frequency of the 2nd order LPF within it must be set by the anti-resonance frequency of the rotor. The rotor system can be stabilized by positive damping due to phase lead for the rigid and 1st bending modes, and due to phase lag with about -270 degree for the higher bending modes. The completed compensator can potentially stabilize all of the bending modes with no material or structure of damping. The effectiveness of this design concept is proven in the experiment using the rotor having one AMB.

This concept is generalized for the rotor borne by two AMBs, as this is a common type, and its effectiveness is made clear by simulation.

REFERENCES

[1] T.Kida, et.al. 2, Optimal Regulator with Low-Pass Property and Its Application to LSS Control, Trans. of the Society of Instrument and Control Engineers (SICE) Vol.25, No.4, p.448-454, (1989-4), (in Japanese)

[2] O.Matsushita et.al, Flexible Rotor Vibration Analysis Combined with Active Magnetic Bearing Control, The International Conference on ROTORDYNAMICS, IFToMM Sep 14-17, 1986, Tokyo, p421

[3] K. Nonami et.al., Spillover Control of Magnetic Levitation Sytem Using H Infinity Control Theory, Trans. of JSME, Vol57, No.534, (1991-2), p.568 (in Japanese)

[4] Y. Tagawa et.al., Modeling and Attitude Control of Flexible Spacecraft, Trans. of JSME, Vol .54, No.507, (1988-11), p.2689 (in Japanese)

APPENDIX

If the LQR method based upon the state feedback control is applied to a control objector composing of the rotor and 2nd LPF, the required compensator of the 3rd order LPF is automatically designed. The corresponding state equation of this enlarged objector as shown in Fig.5 is written by following formulas:

$$\begin{bmatrix} \dot{X} \\ \dot{Z} \end{bmatrix} = \begin{bmatrix} A & bc_F \\ 0 & A_F \end{bmatrix} \begin{bmatrix} X \\ Z \end{bmatrix} + \begin{bmatrix} 0 \\ b_F \end{bmatrix} v$$

$$y = \begin{bmatrix} c & 0 \end{bmatrix} \begin{bmatrix} X \\ Z \end{bmatrix} \qquad (7)$$

$$u = c_F Z$$

where

$$Z = \begin{bmatrix} z \\ \dot{z} \end{bmatrix}$$

$$A_F = \begin{bmatrix} 0 & 1 \\ -\omega_F^2 & -2\zeta_F\omega_F \end{bmatrix}, \quad b_F = \begin{bmatrix} 0 \\ \omega_F^2 \end{bmatrix} \quad \text{and} \quad c_F = \begin{bmatrix} 1 & 0 \end{bmatrix}$$

The application of the LQR generates the following type of control law:

$$G_c(s) = \begin{bmatrix} c_F & 0 \end{bmatrix} \left(sI - \begin{bmatrix} A_F - b_F f_F & -b_F f \\ bc_F & A - kc \end{bmatrix} \right)^{-1} \begin{bmatrix} 0 \\ k \end{bmatrix} \qquad (8)$$

where K_c is the observer gain vector and $[f, f_F]$ the state feedback gain.
An example of the control law obtained by this manner is shown in Fig.6.